Preprint Title Formulation, optimization and *in vitro* evaluation of nanostructured lipid carriers for topical delivery of apremilast

Authors Jyotsana R. Madan, Shweta Khobaragade, Kamal Dua and Rajendra Awasthi

Publication Date 10 Jan 2020

Article Type Full Research Paper

ORCID® iDs Jyotsana R. Madan - https://orcid.org/0000-0001-6663-1890; Rajendra Awasthi - https://orcid.org/0000-0002-1286-1874

Formulation, optimization and *in vitro* evaluation of nanostructured lipid carriers for topical delivery of apremilast

Jyotsana R Madan[1]*, Shweta Khobaragade[1], Kamal Dua[2], Rajendra Awasthi[3]

[1]Department of Pharmaceutics, Smt. Kashibai Navale College of Pharmacy, Savitribai Phule Pune University, Pune, Maharashtra, India, Email: jyotsna.madan@sinhgad.edu,

[2]Discipline of Pharmacy, Graduate School of Health, University of Technology Sydney, Ultimo NSW 2007, Australia, Email: Kamal.Dua@uts.edu.au

[3]Department of Pharmaceutics, Amity Institute of Pharmacy, Amity University Uttar Pradesh, Noida 201313, India , Email: rawasthi1@amity.edu

*Corresponding author

Jyotsana R Madan

Department of Pharmaceutics,

Smt. Kashibai Navale College of Pharmacy,

Savitribai Phule Pune University, Pune, Maharashtra, India;

Email: jyotsna.madan@sinhgad.edu, Tel.: +91-9420148817

ABSTRACT

This work was aimed to formulate topical Apremilast loaded nanostructured lipid-carriers (NLCs) for the management of psoriasis. Psoriasis is a widespread skin condition considered to be a Th1 autoimmune skin disease and characterized by excessive growth and abnormal differentiation of keratinocytes. Objective of the study was to investigate the applicability of lipid matrix of NLC composed of solid lipid and liquid lipid (oil), creating imperfections in the crystal lattice, in improving drug loading as well as physical stability. NLCs were prepared by a cold homogenization technique using Compritol® 888ATO, oleic acid, Tween 80 and Span 20, and Transcutol P as a solid lipid, liquid lipid, surfactant mixture and penetration enhancer, respectively. Carbopol 940 was used to convert NLC dispersion into NLC based hydrogel to improve its viscosity for topical administration. The optimized formulation was characterized for size, polydispersity index, zeta potential, percentage entrapment efficiency (%EE), and surface morphology. Further, viscosity, spreadability, stability, *in- vitro* drug diffusion, *ex-vivo* skin permeation and skin deposition studies were carried out. Apremilast loaded NLCs showed narrow polydispersity index (PDI- 0.339) with particle size of 758 nm, %EE of 85.5% and zeta potential of -33.3 mV. Scanning electron microscopy confirmed spherical shape of NLCs. *In vitro* drug diffusion and *ex vivo* skin permeation results showed low drug diffusion and sustained drug release and 60.1% skin deposition. The present study confirms the potential of the nanostructured lipid form of poorly water-soluble drugs for topical application and increased drug deposition in the skin.

Keywords: Apremilast, cold homogenization, lipid carrier, psoriasis, solid lipids, topical delivery.

INTRODUCTION

Psoriasis is a widespread skin condition considered to be a Th1 autoimmune skin disease. It is characterized by excessive growth and abnormal differentiation of keratinocytes [1]. For the treatment of psoriasis, topical administration is most commonly used in the majority of patients. Any new topical treatment that reduces the dosage and/or frequency of administration of Apremilast (APM) currently being used or can make a currently used treatment more effective, particularly which reduces gastrointestinal related or systemic side effects, is required [2, 3]. However, the challenges associated with psoriatic skin such as skin rigidization, absence of Normal Moisturizing Factors (NMFs) like water and imbalance of skin lipids poses stiff challenge in designing an effective topical delivery system [4]. APM was approved by US FDA for treatment of patients with moderate-to-severe plaque psoriasis and psoriatic arthritis. It is available in the market as an oral formulation and was developed by Celgene Corporation [5]. It may also be useful for other immune system related inflammatory diseases. Unlike TNF-α inhibitors, which bind directly to TNF-α, APM causes a broad inhibition of multiple pro-inflammatory mediators such as interleukin IL-6, IL-10 and TNF-α, exerting therefore an overall anti-inflammatory effect [6]. APM is a BCS (Biopharmaceutical Classification System) class IV drug, which has low permeability and low solubility. Due to this the oral bioavailability of APM is highly variable. Also, the conventional formulations of APM had dose regimen and tolerability issues, which might impair patient compliance and, therefore, the efficacy of the treatment would be compromised [7].

Maintaining the desired concentration of drug at the target site is challenging. Pharmaceutics deals with the development of a drug product which provides a sustained drug release profile. In

the present era, pharmaceutical scientists are more focused on the nanopharmaceutics (a new branch of pharmaceutics) [8] However, it is difficult to control the size of nanoparticles [9]. Various newer techniques such as electrospinning [10-12], electrospray [13], molecular self-assembly [14] have been reported to synthesize nanoformulations. The second generation of lipid nanoparticles *i.e.* nanostructured lipid carriers (NLCs) were developed in 2000s. NLCs consist of different spatial lipids (e.g., glycerides) and thus provide a larger distance between the glycerides' fatty acid chains and general unstructured crystal; and consequently, promote higher drug accommodation [15, 16]. The lipid matrix of NLC is composed of both a solid lipid and a certain amount of a liquid lipid (oil), creating imperfections in the crystal lattice, resulting in improved drug loading capacity as well as physical stability [17, 18]. For several drugs, the solubility in liquid lipid is higher than solid lipid, which enhances drug-loading [19-21]. To prepare APM-loaded NLCs, Compritol® 888ATO (glyceryl behenate) was selected as the solid lipid and lipid-soluble compound oleic acid was chosen as liquid lipid. Recently, Lin *et al*., exploited a dual-active cilomilast loaded NLCs for improved psoriasis therapy and tested their inhibitory capability against human neutrophil stimulation and a murine psoriasis lesion [18]. Choi *et al*., described positively charged NLCs for improving dissolution profile of poorly water soluble drug(s) [22].

Considering the above mentioned physicochemical and biological concerns of APM, challenges associated with psoriatic skin and the merits of NLCs, the aim of this study was to explore the promises of NLCs in the effective delivery of topical delivery of APM. For this, NLCs were synthesized by a cold homogenization method using selected lipids and surfactants. Initially trial formulations were formulated to screen the solid lipids, liquid lipids and surfactants. The

prepared NLCs were characterized for size, polydispersity index, entrapment efficiency, zeta potential, morphology, thermal analysis, X-ray diffraction studies, and stability studies. Finally, the NLCs were incorporated in the gel and the gels were evaluated for viscosity, spreadability, *in vitro* drug diffusion, *ex vivo* skin permeation, and skin deposition.

RESULTS AND DISCUSSION

Preliminary screening of Solid lipids and liquid lipids and surfactants

The lipids showing more solubilization potential for APM were selected for the preparation of NLCs. The solid lipids were ranked by the likely presence of crystals using the microscopic method (Table 1). No crystals were observed in APM-Compritol® 888ATO mixture with the addition of 10 mg APM. Further addition of 30 mg APM to the same mixture, crystals were observed. The highest solubility was observed in Compritol® 888ATO. The results of APM solubility in liquid lipids are presented in Table 2. Oleic acid presented highest solubility (10.301 mg/ml ± 0.658). From saturation solubility of APM in different lipids, it was concluded that Compritol® 888ATO and oleic acid showed higher solubilization potential for APM as compared to other lipids. Thus, these two lipids were selected for further studies.

Solubility data of APM in different surfactants are shown in Table 2. It was observed that, APM presented highest solubility in Tween 80 (34.6 mg/ml ± 0.423). Therefore, Tween 80 was further used for preparation of NLCs.

Table 1: Crystal evaluation by microscopy for APM solubility test.

Crystal rank	Lipid	Soluble at 10 mg/g	Soluble at 30 mg/g	Melting point (°C)
1st	Compritrol® 888ATO	Yes	No	65-66
2nd	Precirol ATO® 5	No	No	50-52
3rd	Apifil®	No	No	59-61
4th	Stearic acid	No	No	69-70
5th	Glyceryl monostearate	No	No	60-62

Table 2: Solubility of APM in liquid lipids and surfactants. The data presents mean ± SD, n = 3.

Liquid lipid	Solubility (mg/ml)	Surfactant	Solubility (mg/ml)
Olive oil	1.315 ± 0.254	Span 80	12.3 ± 0.640
Labrafac Lipophile WL 1349 oil	6.926 ± 0.156	Span 20	15.1 ± 0.37
Linseed oil	7.542 ± 0.258	Tween 40	18.9 ± 0.256
Castor oil	3.564 ± 0.368	Tween 80	34.6 ± 0.423
Oleic acid	10.301 ± 0.658	Kolliphor 188	26.7 ± 0.362
		Kolliphor 64	23.39 ± 0.215

Preliminary trials for the preparation of NLC by the cold homogenization

During preliminary trials, it was observed that the particle size was reduced as the sonication time increased from 10 min to 30 min. Based on literature survey, a blend of hydrophilic and

lipophilic surfactants (Tween 80 and Span 20) was also used during these trials to prepare NLCs (Table 3). The lowest particle size of NLC was obtained for batch A3. It has been reported that using a blend of surfactants prevents particle aggregation, improves physical stability, and promotes particle properties of NLCs [23]. Based on the results of preliminary trials, further experiments were carried out with sonication time fixed for 30 min and using a surfactant mixture of Tween 80 and Span 20 (1:1).

Table 3. Preliminary trials for the preparation of NLCs by cold homogenization method

Batch	**APM (%)**	**Compritol® 888ATO (%)**	**Oleic acid (%)**	**Surfactant (%)**	**Transcutol P (%)**	**Particle size (nm) Sonication time (min)**	
						10	**30**
A1	1	13.5	3	3*	1	2084	1934
A2	1	13.5	3	3**	1	1836	1420
A3	1	13.5	3	3***	1	1526	1360

*Tween 80; **Span 20 and ***Tween 80: Span 20 (1:1)

Experimental design

The two independent variables selected were solid lipid (Compritol® 888ATO) and liquid lipid (oleic acid) and the dependent variable were particle size (PS), entrapment efficiency (% EE). Nine experiments were designed and each variable was tested at 3 designated levels - 1, 0 and +1 (Table 4). The mean particle size and (% EE) (dependent variable) of APM loaded NLCs obtained at various levels of 2 independent variables (X_1 and X_2) were subjected to multiple regression analysis to yield full model second order polynomial equation. Response surface plots

were created to recognize the impact of significant variables utilizing Design-Expert® Software 11.1.2.0.

Table 4: Results of PDI, zeta potential, particle size of apremilast loaded NLCs optimized by 3^2 factorial design

Batch	Compritrol® 888ATO (%) X_1	Oleic acid (%) X_2	Surfactant (%)	Polydispersity Index (PDI)	Zeta Potential (mV)	Particle size (nm)	% EE
F1	+1	-1	3	0.393	-17.7	1603	66.4
F2	+1	0	3	0.187	-18.2	1387	75.4
F3	+1	+1	3	0.192	-18.0	1352	62.3
F4	0	-1	3	0.350	-31.3	817.6	80.7
F5	0	0	3	0.339	-33.3	758	85.5
F6	0	+1	3	0.254	-35.7	803.5	76.6
F7	-1	-1	3	0.326	-20.7	961.2	77.4
F8	-1	0	3	0.393	-20.2	948.5	80
F 9	-1	+1	3	0.283	-20.5	900.7	71.3

All batches contain APM (1%) and Transcutol P (1%); Coded levels: X_1 Compritol® 888ATO (%): (+1): 13.5, (0):12, (-1): 10.5; X_2 oleic acid (%): (+1): 4.5, (0): 3, (-1): 1.5

Actual predicted plot, model summary statistics, fit summary and ANOVA were applied to determine the significance and magnitude of interaction between independent and dependent variables. The regression model was used to generate the contour plots and 3D surface to analyze

interactions of the independent variables [24, 25]. The results of the regression output and response of model summary statistics of APM loaded NLCs are presented in Table 5 and Table 6. The corresponding equations for the model summary statistics are:

Y_1 (PS) = + 760.22 + 255.27X_1 - 54.27X_2 - 47.62X_1X_2 + 401.99X_1^2 + 44.79X_2^2

Y_2 (% EE) = + 85.71 - 4.10X_1 - 2.38X_2 + 0.5000X_1X_2 - 8.52X_1^2 - 7.57X_2^2

where X_1 and X_2 represent the coded values of the Compritol® 888ATO (X_1) and oleic acid (X_2), respectively.

Table 5. The results of model summary statistics

Source	Std. Dev.	R^2	Adjusted R^2	Predicted R^2	PRESS	
Linear	243.46	0.4081	0.2897	-0.1789	1.180E+06	
2FI	254.65	0.4171	0.2229	-1.4808	2.484E+06	
Quadratic	39.20	0.9893	0.9816	0.8912	1.089E+05	Suggested
Cubic	5.97	0.9998	0.9996	0.9793	20708.34	Aliased

The particle size values showed a wide variation ranging from 758 to 1603 nm, while % EE values varied from 62.3% to 85.5%. A significantly higher % EE was achieved in APM loaded NLCs (85.5%) at medium levels (0) of X_1 (12%) and X_2 (3%) in batch F5 and this batch showed particle size of 758 nm.

Table 6. The results of fit statistics

Std. Dev.	39.20	**R^2**	0.9893
Mean	966.42	**Adjusted R^2**	0.9816
C.V. %	4.06	**Predicted R^2**	0.8912
Adeq precision			30.5415

Effect of Compritol® 888ATO and oleic acid on particle size

The response surface plot and the contour plot signify the effect of the amount of Compritol® 888ATO (X_1) and the oleic acid (X_2) on the response Y_1 (particle size) (Fig. 1 A and B). Compritol® 888ATO concentration had a positive effect on particle size. As the concentration of oleic acid increases from 1.5% to 3.0%, particle size decreases, further increase of oleic acid to 4.5% leads to no further decrease in particle size. This may be due to liquid lipid being excluded during the particle formation. As soon as the system is cooled, lipid starts solidifying and arranges itself as a nanoparticle, whereas liquid lipid because of its soft structure may remain outside or randomly distributed [26]. The response surface plot and the contour plot signify the effect of the amount of Compritol® 888ATO (X_1) and the oleic acid (X_2) on the response Y_2 (% EE). As the concentration of Compritol® 888ATO increases from 10.5% to 12.0%, % EE also increases. Further increase of Compritol® 888ATO to 13.5% does not enhance the % EE (Fig. 1 C and D).

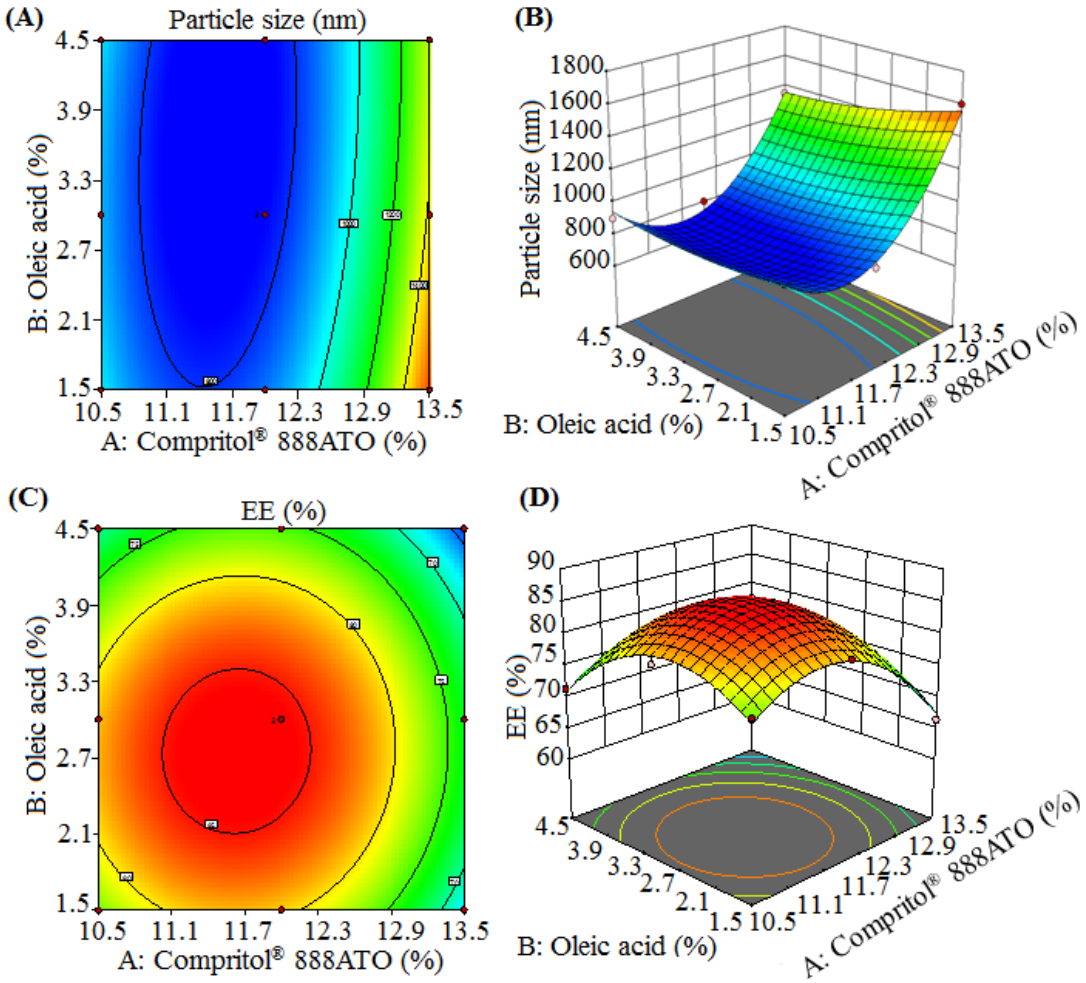

Fig. 1 Contour plots and response surface plots showing the influence of Compritol® 888ATO (X_1) and oleic acid (X_2) particle side (A and B), and entrapment efficiency (C and D)

Characterization of NLC dispersions

Particle size and polydispersity index

The amount of lipid had a great effect on particle size, since a small increase in amount of lipid increased particle size drastically. An increase in liquid lipid content decreased particle size. Small particle size is considered potentially useful for the delivery of drugs through the skin. The PDI $\leq$ 0.5 value indicates that the formulation had a narrow range size distribution. The usual

diameter of NLCs ranges from 10 to 1000 nm. A particle size higher than 300 nm provides sustained drug delivery, whereas the particles in the size range between 50 to 300 nm displayed rapid release [27]. Based on the factorial design studies, batch F5 with particle size 758 nm (Fig. 2) was selected for further loading into hydrogel.

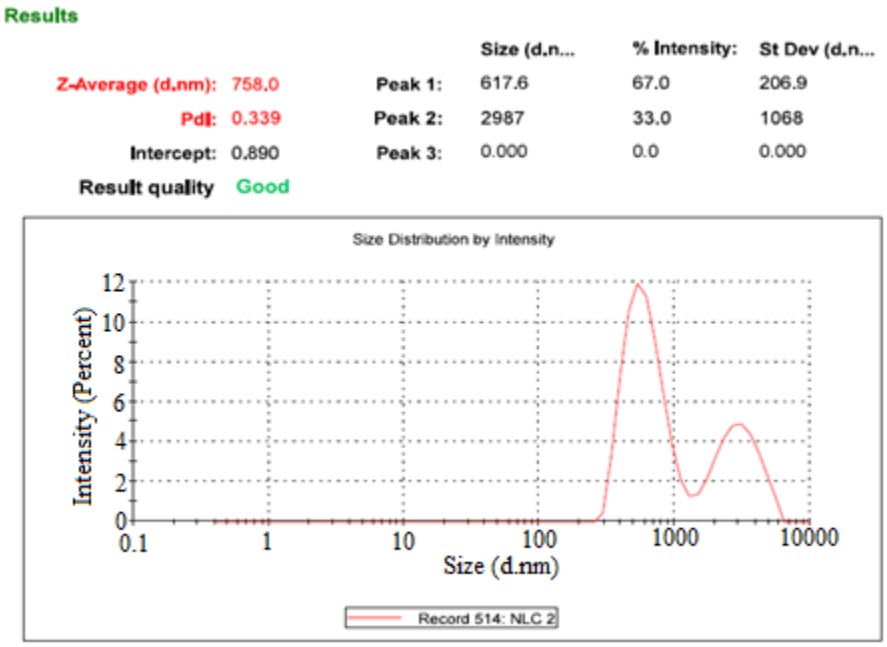

Fig. 2 Particle size of APM loaded NLCs (F5 batch)

Entrapment efficiency

The % EE of various APM batches was observed to be in the range of 62.3 to 85.5% (Table 4). The entrapment efficiency increased with an increase in the concentration of both solid lipid and liquid lipid up to a certain level. During the formulation process, the lipid particles are cooled to crystallize and form solid particles. The two lipids Compritol® 888ATO and oleic acid being spatially different, when mixed together create imperfections in the crystal order of the lipids leading to increased distance between fatty acid chains in the matrix structure of Compritol® 888ATO [28, 29]. Therefore, the formed matrix contains various deformities proposing more

space to incorporate APM. Results show that the formulation containing Compritol® 888ATO (12.0% w/w) and oleic acid (3.0% w/w) had highest % EE (batch F5).

Zeta potential (ZP)

The estimation of zeta potential predicts the stability of colloidal dispersions. In the present study, the zeta potential values ranged from -17.7 to -35.7 mV, indicating good physical study. NLC dispersion (Batch F5) which shows the highest entrapment efficiency (85.5%) and lowest particle size (758 nm) has a zeta potential of -33.3 mV (Fig. 3). This indicates a strong electrostatic repulsion, rendering the formulation stable [30].

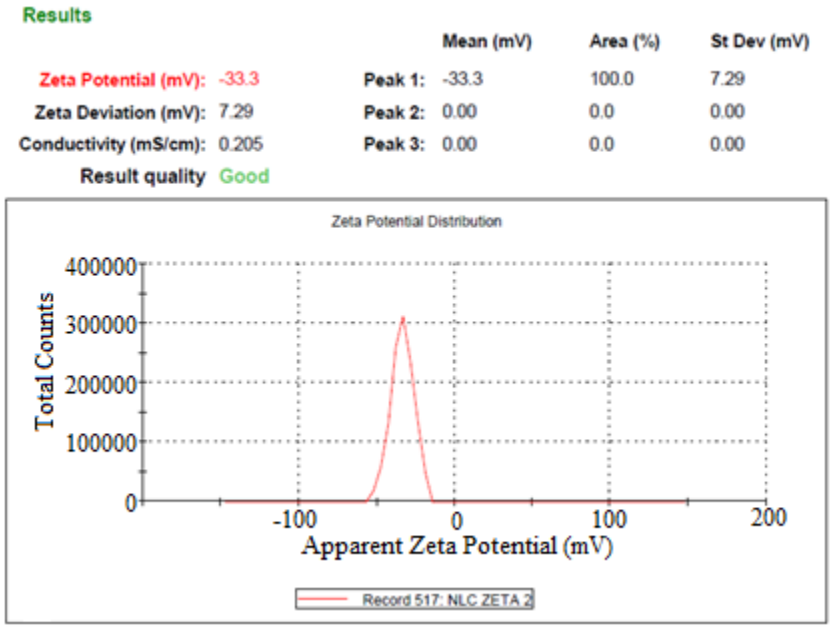

Fig. 3 Zeta Potential of APM loaded NLCs (batch F5)

Morphological characterization

Fig. 4 shows the SEM image of NLC dispersion (batch F5) indicating spherical shape and nano size of the particles.

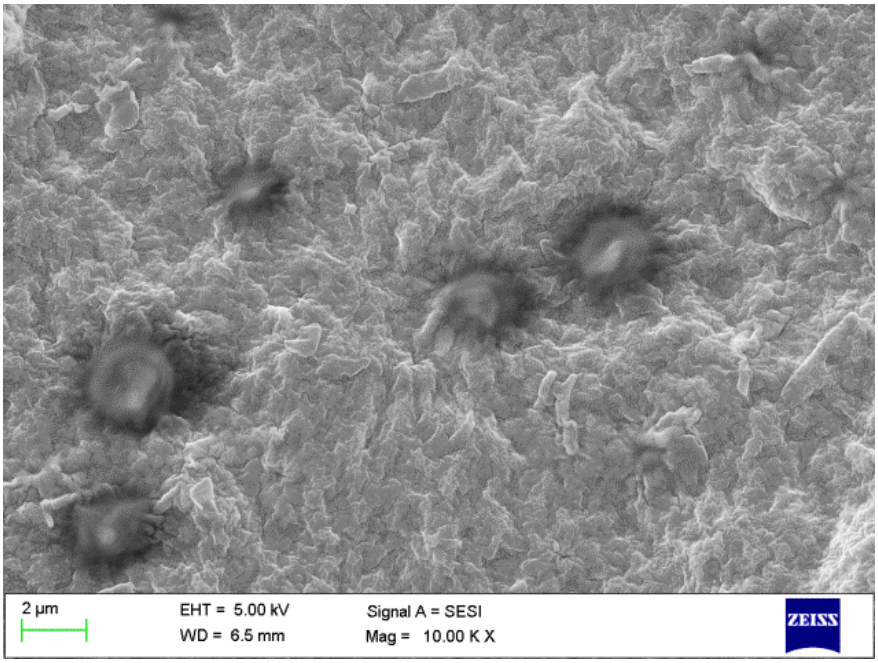

Fig. 4 Scanning electron micrograph of APM loaded NLC (batch F5)

Fourier-transform infrared study

The FTIR spectra of pure APM, PM, and lyophilized NLCs (batch F5) are presented in Fig. 5. The FTIR spectrum of pure APM showed characteristic peak of N–H stretching at 3364 cm^{-1}. Characteristic peak at 1764 cm^{-1} in the spectrum of pure APM due to amide carbonyl (C=O), along with the peaks between 2837 cm^{-1} and 3003 cm^{-1} for aliphatic and aromatic benzene ring C–H stretching. The peak for amide N–H bending was observed at 1519 cm^{-1} and the peak for C–O stretching was observed at 1233 cm^{-1}. All the characteristic peaks of APM were present in the spectrum of PM and lyophilized NLCs (batch F5). However, the intensity of the characteristic peaks of APM was decreased in the spectrum of PM and lyophilized NLCs. This suggests that there are no chemical interactions between APM and lipids [31].

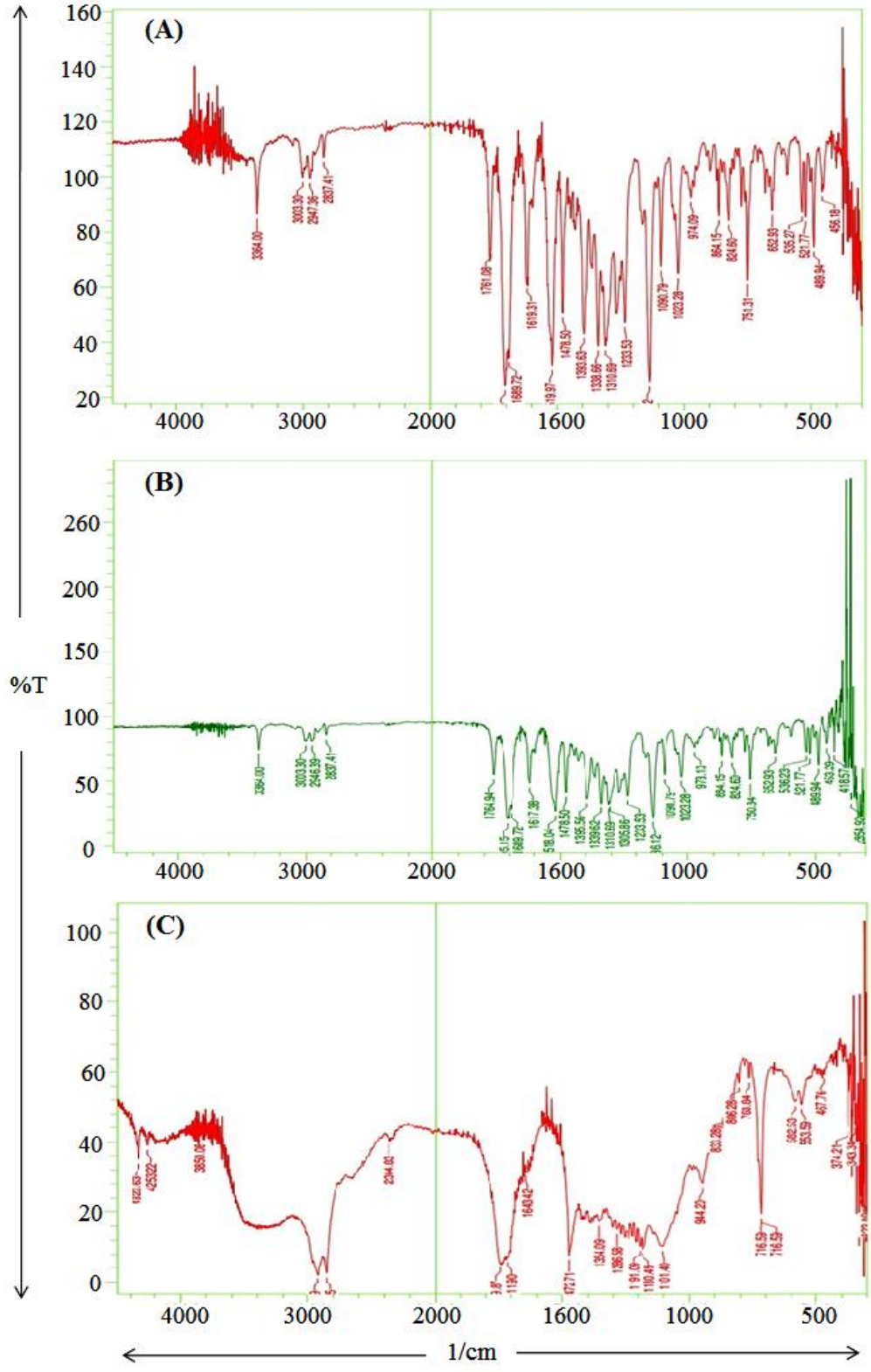

Fig. 5 FTIR spectrums of pure APM (A), PM (B), and Lyophilized NLCs (batch F5)

Thermal analysis

DSC thermogram gives the information about crystalline or amorphous nature of the drug. In the thermogram of pure APM, endothermic peak at 159.56 °C (δ at 111.877 J/g) was recorded corresponding to melting melting range from 155.01ºC to 159.56ºC (Fig. 6 A). The peak at 70.19°C (δ 112.367 J/g) in the thermogram of Compritol® 888ATO corresponding to its melting peak ranges from 67.27 °C to 71.49 °C (Fig. 6 B). The thermogram of physical mixture showed two discrete endothermic events, the first endothermic event in the broad range between 68.62°C and 72.23°C (δ 60.191 J/g) and the second endothermic event between 151.18°C and 157.62°C (δ 29.437 J/g) (Fig. 6C). A slight shift in the APM peak was recorded in the thermogram of PM which may be due to the interaction of the APM with the lipid matrix. The DSC thermogram presented in Fig. 6 (D) demonstrates the disappearance of APM peak in the formulation (NLC) which suggesting that the drug is completely enclosed inside the lyophilized NLCs.

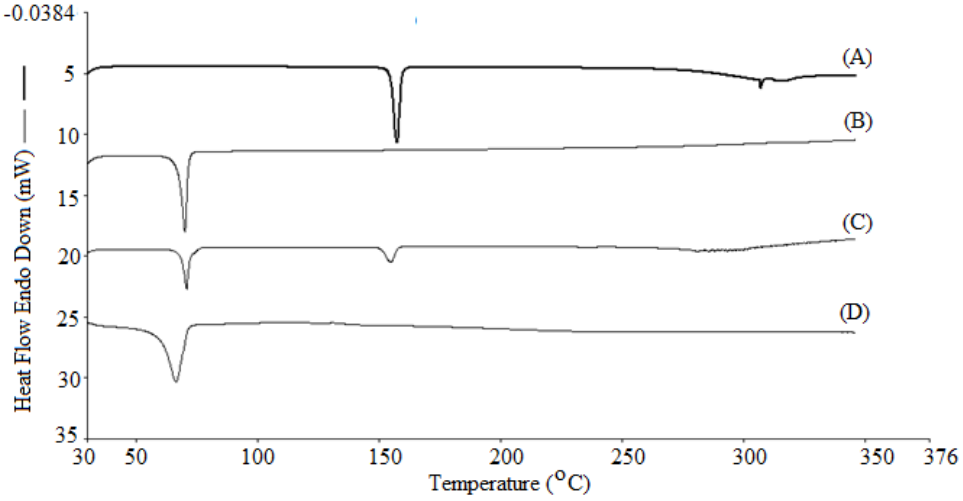

Fig. 6 Differential scanning calorimetry of pure APM (A), Compritol® 888ATO (B), PM (C) and lyophilized NLCs (batch F5) (D)

X-ray diffraction studies (XRD)

APM powder is highly crystalline in nature, as clear from sharp peaks observed in the x-ray spectrum. Fig. 7 shows the XRD spectrums of pure APM, PM and lyophilized NLCs (batch F5). The characteristic diffraction peaks were observed at 21.12°, 27.29°, 26.44°, 12.61°, 13.70°, 16.50° and 24.99° in the diffractogram of pure APM. The deformed peaks in the NLCs confirm amorphous form of APM in the NLCs. The crystalline state of APM in the PM of Compritol® 888ATO and APM is apparent from the characteristic diffraction peaks. The reduced peak intensity in the NLC indicates reduction in crystallinity due to incorporation of APM into NLCs. Thus, the XRD pattern of the NLCs ascertains the amorphous structure of APM in the formulation [32].

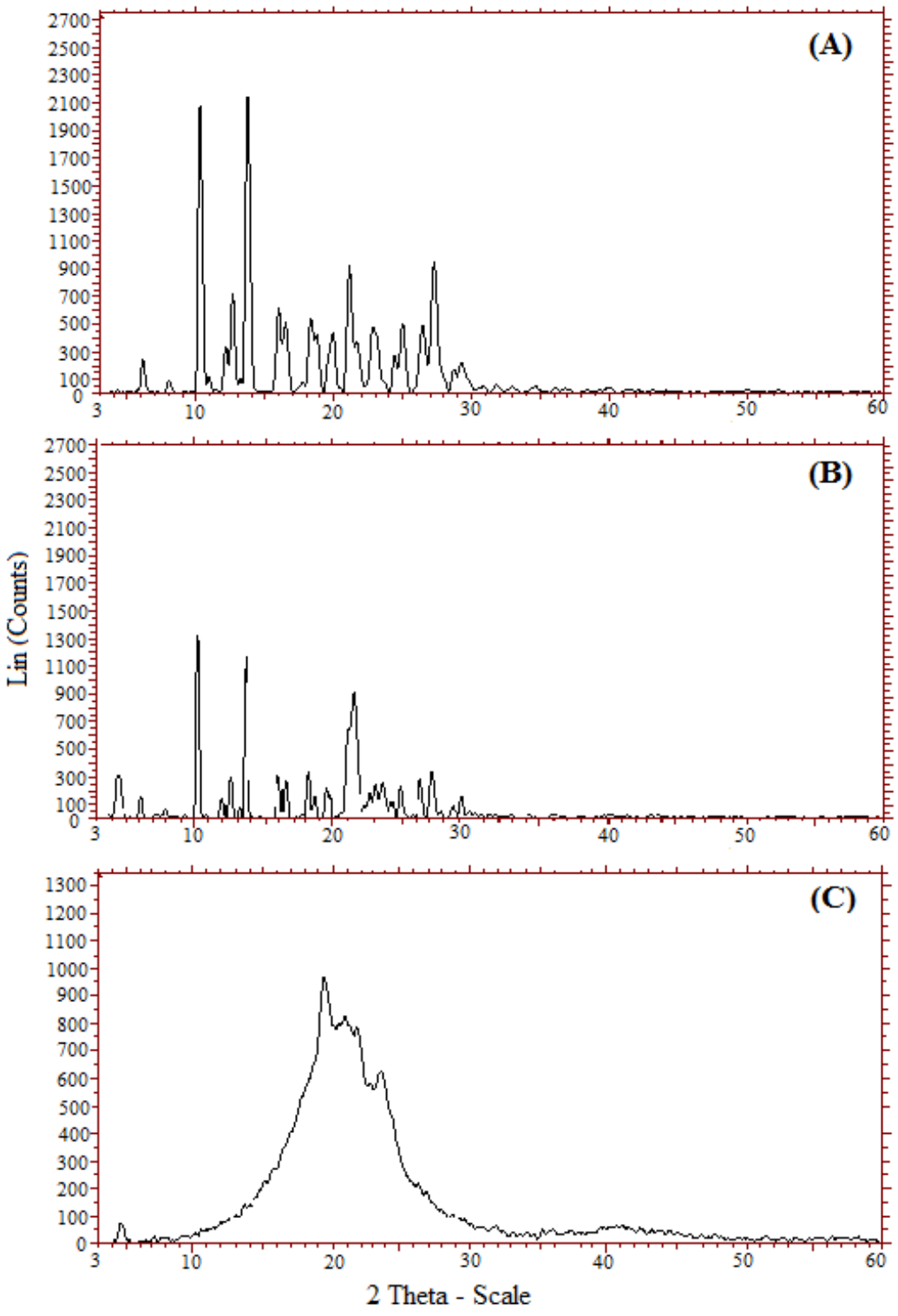

Fig. 7 X-ray diffraction patterns of pure APM (A), physical mixture (B), and lyophilized NLCs (batch F5)

Stability studies

Stability studies of NLC dispersion (batch F5) were carried out at different temperature conditions like stored at refrigerated temperature (4 ± 2°C), room temperature (25 ± 2°C) and hot humid temperature (45 ± 2°C) for 3 months to evaluate phase separation and entrapment efficiency. The entrapment efficiency of NLC dispersion (batch F5) were found to be 85.5 ± 0.235, 77.8 ± 0.157, 85.2 ± 0.364, and 72.6 ± 0.125, respectively at 4 ± 2°C, 25 ± 2°C and 45 ± 2°C (Table 7). No phase separation was observed.

Table 7. Stability data of NLC dispersion (batch F5). The data presents mean ± SD (n = 3).

Storage conditions	**Time (days)**	**%EE**	**Phase separation**
Control	0	85.5 ± 0.235	No
Refrigerated temperature (4 ± 2°C)	90	77.8 ± 0.157	No
Room temperature (25 ± 2°C)	90	85.2 ± 0.364	No
Hot humid temperature (45 ± 2°C)	90	72.6 ± 0.125	No

Evaluation of APM loaded NLCs based hydrogels

The prepared gel containing NLC dispersion (batch F5) was white, smooth and homogenous with semisolid. The formulation had viscosity of 6000 cps and pH of 6.5. Texture profile analysis spectra of APM loaded NLC hydrogel (batch F5) showed the hardness of 164.80 ± 0.235 g, adhesive force of 63.30 g, and adhesiveness of 5.29 mJ. The values indicate good spreadability characteristics.

In-vitro drug diffusion studies

For drug release studies, phosphate buffer (pH 6.8) and methanol mixture (80:20) was selected as the receptor media based on solubility profile of the drug. The percentage drug diffusion of pure APM loaded gel, NLC dispersion (batch F5) and NLCs based hydrogel was analyzed over a period of 8 h. For better patient compliance, an ideal topical formulation should show sustained release for a longer period. The percentage drug diffused from NLC dispersion (batch F5) and NLCs based hydrogel was found to be low, this can be attributed to the high lipid content encapsulating the drug and reducing its partition in the outer phase and consequently its release in the receptor media [33]. Furthermore, NLCs based hydrogel showed slower diffusion of the drug as compared to NLC dispersion due to the high viscosity of gel and presence of hydrogel matrix (Fig. 8).

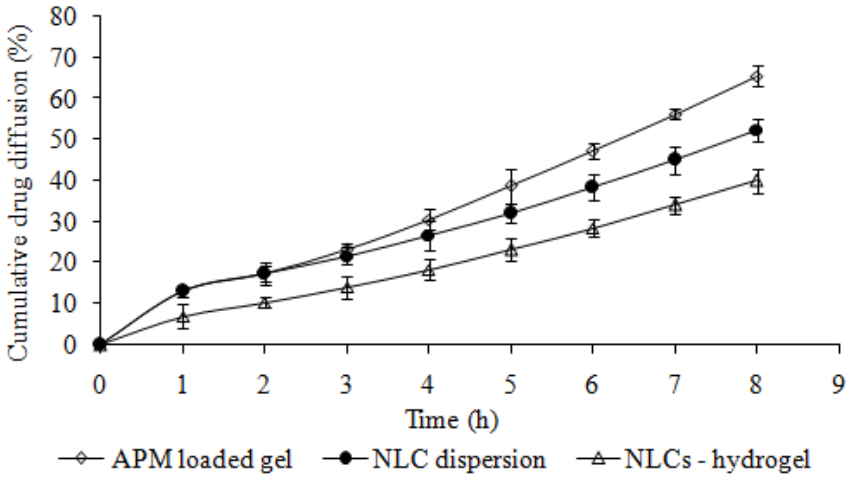

Fig. 8 Cumulative percent drug diffusion from APM loaded gel, NLC dispersion and NLC based hydrogels. The data presents mean ± SD (n = 3). The drug concentration in APM-NLCs loaded gel and hydrogel is 0.3% w/w and in NLC dispersion is 1% w/w.

Ex -vivo skin permeation study

Treatment of psoriasis can be supported by formulations that have minimum permeation and maximum skin deposition of the drug. The percentage drug permeated from pure APM loaded gel, NLC dispersion (batch F5) and NLCs based hydrogel was studied over a period of 24 h. The NLCs based hydrogel exhibit 48.72 ± 0.848% permeation and NLC dispersion demonstrated 62.17 ± 0.249% of drug permeation in 24 h. Both NLC dispersion and NLCs based hydrogel show slow drug release. Permeation parameters like steady state flux (J_{ss}) and permeability coefficient (K_p**)** were also calculated (Table 8). Low flux values obtained for the NLCs based hydrogel indicated sustained release effect.

Table 8. Results of permeability study.

Parameters	**Flux (µg/cm^{2}h^{-1})**	**Permeability coefficient (cm^{-2}/h^{-1})**
Pure APM loaded gel	28.767	1.856
NLC dispersion	20.9295	1.655
NLCs based hydrogel	18.929	1.557

Skin deposition studies

APM loaded NLCs based hydrogel showed 60.1% skin deposition (Fig. 9). Psoriatic skin is very critical to treat due to the hyper-proliferation of the epidermal keratinocytes and needs a topical formulation and not transdermal. As per the requirement of an ideal formulation, higher deposition of drug in epidermal skin and minimal permeation through the skin is required to

release the drug for a longer period after application. Thus, the NLCs based hydrogel formulation was found to be ideal for the topical application for psoriasis [34].

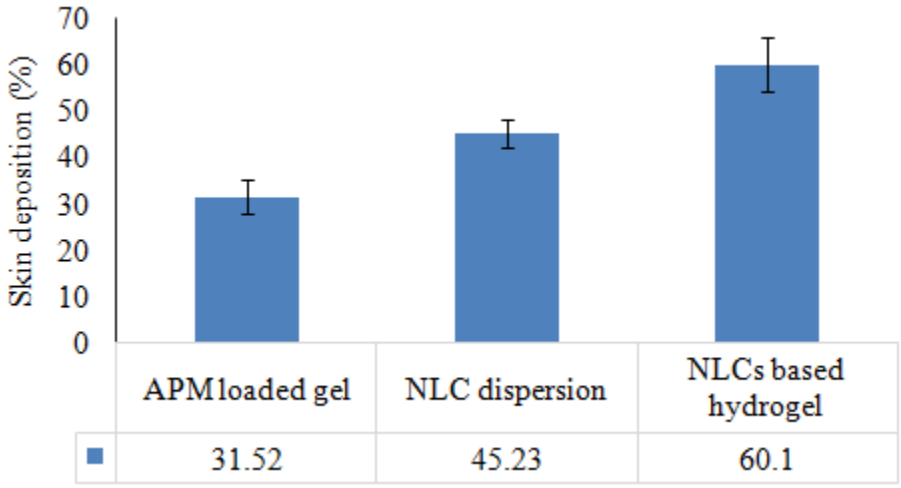

Fig. 9 Results of percentage skin deposition study. The data presents mean ± SD (n = 3). The drug concentration in APM-NLCs loaded gel and hydrogel is 0.3% w/w and in NLC dispersion is 1% w/w.

MATERIALS AND METHODS

Materials

APM was gifted by Glenmark Pharmaceuticals Ltd., Nashik, India. Glycerol monostearate (GMS), Compritol® 888ATO, Apifil®, Precirol ATO 5, Labrafac Lipophile WL 1349 oil and Transcutol® P were gifted by Gattefosse India Pvt. Ltd., Mumbai, India. Stearic acid, Tween 80, Tween 40, Span 20, Span 80, olive oil, castor oil, linseed oil, oleic acid, Carbopol® 940P, and propylene glycol were purchased from Research Lab Fine Chem Industries, Mumbai, India. Methanol was gifted by Thomas Baker Chemicals Pvt. Ltd., Mumbai, India. Kolliphor 64 and Kolliphor 188 were provided by BASF India Ltd., Mumbai, India.

Methods

Preformulation study

Preliminary screening of solid lipids

The saturation solubility of APM in different lipids was determined using the microscopic method [19]. Briefly, 10 mg of APM was added to the solid lipid and heated 10°C above the melting point of lipid and agitated for 24 h utilizing magnetic stirrer with hot plate (1 MLH, Intex, Mumbai India). Samples were taken and observed under an optical microscope at 10X magnification (BA210 Labomed, Hong-Kong, China). The APM concentration was balanced to obtain crystals. The outcomes were ranked based on the amount of crystals formed. The higher position in the rank indicated the formation of lower amount of crystals.

Preliminary screening of liquid lipids and surfactant

The solubility of APM in various liquid lipids and surfactants was determined by adding excess amount of APM in 5 ml of each of the lipid or surfactant in a glass vials. To achieve equilibrium, the vials were stirred at 50 rpm using a magnetic stirrer (1 ML, REMI Instruments Division, Mumbai, India) and kept at 37 ± 1.0°C for 24 h. The vials were centrifuged (RM-12C, REMI Instruments Division, Mumbai, India) at 1500 rpm for 30 min. The samples were filtered through 0.45 μm membrane filter using vacuum filtration. To determine the APM, supernatant was suitably diluted with methanol and analyzed at 230 nm using a UV spectrophotometer (V-730, Jasco, Japan) [35].

Preliminary trials for the preparation of NLCs

APM loaded NLCs were prepared using cold homogenization method, with the selected lipids (Compritol® 888ATO and oleic acid) and surfactants (Tween 80 and Span 20 individual or combination at 1:1 ratio). Briefly, Compritol® 888ATO and oleic acid were melted. To the molten lipid mass, APM, surfactant and penetration enhancer (Transcutol P) were dispersed and stirred. The mixture was sonicated for a specific time period using Probe Sonicator (Sonapros PR-250, Oscar Ultrasonics, Mumbai) (Table 3). The mixture was cooled quickly by putting in an ice bath. The APM-containing solid lipid mass was pulverized to microparticles using a clean and dry mortar and pestle. Microparticles were subsequently dispersed into an aqueous solution of propylene glycol (2% v/v) at 4 ºC (the final volume was 30 mL) [36, 37].

Experimental design

A 3^2 factorial design was applied for the determination of effect of independent variables. The amount of Compritol® 888ATO (X_1) and concentration of oleic acid (X_2) were selected as independent variables. Particle size (nm) (Y_1) and % entrapment efficiency (% EE) (Y_2) were selected as dependent variables. Various models, such as linear, 2FI (Two factor interaction) cubic and quadratic were fitted to the data for two responses simultaneously using Design Expert Software (11.1.2.0, Stat-Ease Inc., USA). The experimental design with corresponding formulations is presented in Table 5.

Statistical analysis

The information is expressed as the mean ± standard deviation. The statistical analysis was finished utilizing Design master software 11.1.2.0. ANOVA repeated measures analysis of

variance was used to assess the significance of the difference between quantitative variables. $P < 0.05$ was statistically significant. Focus was on the model maximizing the adjusted R^2 and the predicted R^2.

Characterization of NLC dispersions

Determination of particle size and polydispersity index

Particle size (z-average diameter) and polydispersity index (PDI) were measured using Malvern Zetasizer Nano ZS 90 (Malvern Instruments, UK) at 25°C. The NLC dispersion was appropriately diluted (particle count rate between 100 and 1000 s^{-1}) with double-distilled water before measurement [38].

Determination of entrapment efficiency (% EE)

The formed NLCs containing APM were separated by centrifugation (RM-12C, REMI Instruments Division, Mumbai, India) at 15000 rpm for 45 min. The supernatant was recovered and assayed spectrophotometrically using a UV spectrophotometer (V-730, Jasco, Japan) at 230 nm against methanol as blank [39]. The % EE of drug was calculated using following formula:

$$\text{Entrapment efficiency (\%)} = \frac{\text{Wt. of initial drug} - \text{Wt. of free drug}}{\text{Wt. of initial drug}} \times 100$$

where Wt. of initial drug is the initial drug amount used for the formulation of NLCs and Wt. of free drug is the free APM amount detected in the supernatant after centrifugation of the aqueous dispersion.

Determination of zeta potential (ZP)

Zeta potential was determined by the measurement of the electrophoretic mobility utilizing a Malvern Zetasizer Nano ZS 90 (Malvern Instruments, UK).

Morphological characterization

The surface morphology of APM loaded NLCs was studied using scanning electron microscopy (SEM) (Carl Zeiss AG, Oberkochen, Germany). Before observation, the samples were mounted on metal grids and coated with silver under argon atmosphere using a high vacuum evaporator (Polaron SEM coating system).

Fourier-transform infrared (FTIR) spectroscopy

The NLC dispersion (batch F5) was lyophilized (Labconco, Free Zone 2.5 plus, Missouri, USA) and used for FTIR examination. The FTIR spectrum of pure APM, physical mixture of APM with Compritol® 888ATO (PM) and lyophilized NLCs (batch F5) were recorded over a range of 4000-400 cm^{-1} to distinguish atomic structures and components using FTIR spectrophotometer (IR Prestige-21, Shimadzu Corp., Tokyo, Japan) by potassium bromide disc method [40].

Thermal analysis

Thermal characteristics of pure APM, PM and lyophilized NLCs (batch F5) were evaluated using differential scanning calorimetry (DSC 4000, Perkin Elmer, Massachusetts, United States). The samples were placed in aluminum pans. An empty aluminum pan was used as a reference. The

DSC measurements were carried out at a heating rate of 10°C/min from 30°C to 300°C under nitrogen atmosphere (20 ml/min) [41].

X-ray diffraction studies (XRD)

XRD study was performed to analyze physical form (crystalline or amorphous) of the APM in APM loaded NLCs. X-ray powder diffraction studies of pure APM, PM and lyophilized NLCs (batch F5) were carried out using x-ray diffractometer (D8 Advance, Bruker, Massachusetts, United States). The samples were analyzed over 0-50° of the diffraction angle (2 Theta). The samples were smeared over low background sample holder (amorphous silica holder) and fixed on the sample stage in goniometer. The instrument was set with B-B geometry. The current and voltage were set to 35 mA and 40 mV, respectively.

Stability studies

The stability study of NLC dispersion (batch F5) was carried out according to the ICH Q1A (R_2) guidelines at different storage conditions *viz.,* refrigerated temperature, room temperature and hot humid temperature. The stability of optimized APM NLCs based hydrogel was assessed for 90 days depending on % EE and phase separation [42].

Preparation of hydrogels

For the preparation of hydrogel, Carbopol 940 (1% w/w) was dispersed in purified water. The mixture was stirred for 10 min at 1500 rpm using a magnetic stirrer, and immediately neutralized with triethanolamine to get pH 6.5. Hydrogels were further allowed to equilibrate for 24 h at room temperature and NLCs (batch F5) were dispersed into the gel. The final concentration of

APM in the gel was 0.3% w/w. The gel was kept overnight to remove entrapped air [43]. A similar procedure was followed for the preparation of the pure APM loaded hydrogel (0.3% w/w).

Evaluation of NLCs based gel containing APM

The formulations were observed for their visual appearance, odor, color and feel upon application such as grittiness, consistency and pH. The pH of each gel batch was determined using a calibrated pH meter (EQ-610, Equip-Tronics, Mumbai, India). One gram of each gel formulation was dispersed in 30 mL of distilled water. The pH was recorded by bringing the electrode near the surface of the formulations and allowing it to equilibrate for 1 min.

Determination of viscosity

The viscosity determinations were carried out using a small sample adapter for Brookfield viscometer (DV II, Brookfield, USA). The 15 ml of formulation was sheared at a rate of 50 rpm/min utilizing spindle no. 62 at room temperature. Viscosity measurement for each sample was carried out in triplicate [44].

Spreadability

Spreadability of the APM loaded hydrogel was examined utilizing a CT V1.7 texture analyzer (Brookfield Engineering Lab, Inc., USA) in the TPA mode [45].

In vitro drug diffusion studies

In vitro release of APM from different NLCs gel formulations was evaluated using dialysis membrane technique. *In vitro* drug release studies were performed on Franz diffusion cell (Orchid Scientifics, Nashik, Maharashtra, India) [46]. Ten milligrams of each formulation *i.e.* APM loaded hydrogel, NLC dispersion (batch F5) and NLC based hydrogel were placed on one side of the dialysis membrane-110 LA 395-1MT (2 x 2 cm, molecular weight cut off: 1200 - 14,000 Dalton; HiMedia Laboratories Pvt. Ltd., Mumbai, India) using 5 mL of phosphate buffer (pH 6.8) and methanol mixture (80:20) as release media stirred at 50 rpm. The temperature was maintained at 37±0.5 ºC. Sampling was carried out at predetermined intervals (0, 0.25, 0.5, 1, 2, 3, 4, 5, 6, 7 and 8 h) from the receptor media and replaced with the equal volume of the fresh solvent [47]. The samples were then filtered and assayed for drug content after suitable dimensions.

Ex vivo skin permeation studies

Ex vivo skin permeation studies were carried out using Franz diffusion cell on full thickness rat stomach skin. Ethical clearance of the animal experimental protocol was obtained from institutional animal ethical committee of Smt. Kashibai Navale College of Pharmacy, Savitribai Phule Pune University, Pune, Maharashtra, India (IAEC-122-19/2019). The hairs were expelled from the extracted skin and subcutaneous fat was removed with a surgical tool. The skin was cleaned with methanol and further washed with distilled water. The skin was mounted on the Franz diffusion cell. The receptor chamber with cross-sectional region of 2.2 cm^2 was loaded up with 5 ml of diffusion medium phosphate buffer (pH 6.8) and methanol mixture (80:20). A small quantity of test gel (10 mg) was uniformly applied on dorsal side of the rat skin. The receptor chamber was stirred at 100 rpm at temperature of 37±0.5°C. The samples (2 ml) were withdrawn

from the receptor compartment at predetermined time intervals (0, 0.25, 0.5, 1, 2, 4, 6, 8, 10,12, 15, 18 and 24 h) and immediately replaced with fresh diffusion medium maintained at the same temperature [48]. The sampling was carried out in triplicate. The samples were analyzed using UV-Vis spectrophotometer (V-730, Jasco, Japan) at 230 nm. Flux ($\mu g/cm^2h^{-1}$) and permeability coefficient (Pb) [cm^{-2}/h^{-1}] were determined using following formula:

$$J = \frac{dQ}{dt\,A}$$

where, J = flux ($\mu g/cm^2\ h^{-1}$), dQ/dt = Slope obtained from linear curve, A = Area of diffusion (cm^2)

The permeability coefficient (Pb) was calculated by dividing J with initial concentration of the drug in the donor cell (CO) by using following formula:

$$Pb = \frac{J}{CO}$$

Skin deposition studies

This study was performed after completion of *ex-vivo* skin permeation study. For the determination of drug deposited in the skin, Franz diffusion cell was dismounted after a time of 24 h. The skin was carefully removed from the cell. The gel applied on skin surface was swabbed with phosphate buffer (pH 6.8) followed by methanol. The procedure was repeated twice to ensure traces of formulation are not left onto the skin surface. The skin was cut into little pieces and kept in methanol to extract the drug present in skin for 48 h. The resulting mixture was filtered and the filtrate was diluted with methanol and analyzed using UV-Vis

spectrophotometer (Jasco V-730, Japan) to determine the amount of drug deposited in the skin [49].

CONCLUSION

In the present study an attempt to formulate APM loaded NLCs was made by utilizing a cold homogenization method using Carbopol 940 as gelling agent. NLCs were prepared utilizing varying concentrations of solid lipid and liquid lipid. NLCs (batch F5) showed great physical stability, a high entrapment efficiency value, lower particle size and sustained drug release. NLCs showed slow and prolonged release profile to maintain the concentration of drug over the skin. The NLC gel had good consistency, homogeneity, spreadability and stability. The present study confirms the potential of the nanostructured lipid form of poorly water-soluble drugs for topical application and increased drug deposition in the skin.

CONFLICT OF INTEREST: The authors declare that they have no conflict of interest.

REFERENCES

1. Madan, J.; Dua, K.; Khude, P.; *Int J Pharm Investig*, **2014,** 4(2), 60-64.
2. Jaya, A.; Mishra, V.; Chaudhari, K.; Mittal, V. Topical compositions of apremilast. WO patent application 2017/216738 A1, 21 December, **2017**.
3. Sreedharala, V. N. Apremilast pharmaceutical compositions. WO patent application 2017/168433 Al, 5 October 2017.
4. Katare, O. P.; Raza, K.; Singh, B.; Dogra, S. *Indian J Dermatol Venereol Leprol*, **2010,** 76(6), 612.

5. Poole, R. M.; Ballantyne, A. D. *Drugs*, 2014, 74(7), 825-837.
6. Tang, M.; Hu, P.; Huang, S.; Zheng, Q.; Yu, H.; He, Y. *Chem Pharm Bull*, 2016, 64(11), 1607–1615.
7. Anwer, M. K.; Mohammad, M.; Ezzeldin, E.; Fatima, F.; Alalaiwe, A.; Iqbal, M. *Int J Nanomed*, **2019,** 14, 1587–1595.
8. Yang, Y.; Zhu, T.; Liu, Z.; Luo, M.; Yu, D. G.; Bligh, S. A. *Int J Pharm*, 2019a, 569, 118634.
9. Huang, W.; Hou, Y.; Lu, X.; Gong, Z.; Yang, Y.; Lu, X. J.; Liu, X. L.; Yu, D. G. *Pharmaceutics*, **2019,** 11(5), 226.
10. Zhou, H.; Shi, Z.; Wan, X.; Fang, H.; Yu, D. G.; Chen, X.; Liu, P. *Nanomaterials*, **2019,** 9(6), 843.
11. Wang, M.; Hai, T.; Feng, Z.; Yu, D. G.; Yang, Y.; Annie Bligh, S. W. *Polymers*, **2019,** 11(8), 1287.
12. Yang, Y.; Li, W.; Yu, D. G.; Wang, G.; Williams, G. R.; Zhang, Z. *Carbohydr Polym*, **2019b,** 203, 228-237.
13. Wang, K.; Wen, H. F.; Yu, D. G.; Yang, Y.; Zhang, D. F. *Materials & Design*, **2018,** 143, 248-525.
14. Yang, C.; Yu, D. G.; Pan, D.; Liu, X. K.; Wang, X.; Bligh, S. A.; Williams, G. R. *Acta Biomaterialia*, **2016,** 35, 77-86.
15. Mukherjee, S. Indian J Pharm Sci, **2009,** 71(4), 349-358.
16. Mishra, V.; Bansal, K.; Verma, A.; Yadav, N.; Thakur, S.; Sudhakar, K.; Rosenholm, J. Pharmaceutics, **2018,** 10(4), 1–21.

17. Ding, Y. Lipid nanoparticles for topical delivery: solid lipid nanoparticles (SLN) & smart Lipids. Thesis (PhD). Freie Universität Berlin 2018.
18. Lin, C. Y.; Hsu, C. Y.; Elzoghby, A. O.; Alalaiwe, A.; Hwang, T. L.; Fang, J. Y. Acta Biomaterialia, **2019,** 90, 350-361.
19. Patel, D.; Dasgupta, S.; Dey, S.; Roja Ramani, Y.; Ray, S.; Mazumder, B. Sci Pharm, **2012,** 80(3), 749–764.
20. Müller, R. H.; Petersen, R. D.; Hommoss, A.; Pardeike, J. Adv Drug Deliv Rev, **2007,** 59(6), 522–530.
21. Souto, E. B.; Müller, R. H. J Microencapsul, **2005,** 22(5), 501–510.
22. Choi, K. O.; Choe, J.; Suh, S.; Ko, S. Molecules, **2016,** 21(5), 672.
23. Monteiro, L. M.; Löbenberg, R.; Cotrim, P. C.; Barros de Araujo, G. L.; Bou-Chacra, N. Biomed Research International, **2017,** 9781603, 1-11.
24. Gaba, B.; Fazil, M.; Khan, S.; Ali, A.; Baboota, S.; Ali, J. Bull Fac Pharmacy, Cairo Univ, **2015,** 53(2), 147–159.
25. Zadeh, S. M. B.; Niro, H.; Rahim, F.; Esfahani, G. Sci Pharm, **2018,** 86(2), 16.
26. Gardouh, A. R.; Faheim, S. H.; Noah, A. T.; Ghorab, M. M. Int J Pharm Pharm Sci, **2018,** 10(4), 61-75.
27. Souto, E. B.; Wissing, S. A.; Barbosa, C. M.; Müller, R. H. Eur J Pharm Biopharm, **2004,** 58(1), 83–90.
28. El-Housiny, S.; Shams Eldeen, M. A.; El-Attar, Y. A.; Salem, H. A.; Attia, D.; Bendas, E. R.; El-Nabarawi, M. A. Drug Deliv, **2018,** 25(1), 78–90.
29. Madan, J. R.; Pawar, A. R.; Patil, R. B.; Awasthi, R.; Dua, K. Polym Med, **2019,** 48(1), 17–24.

30. Madan, J. R.; Ghuge, N. P.; Dua, K. Drug Deliv Transl Res, **2016,** 6(5), 511–518.

31. Araújo, J.; Gonzalez-Mira, E.; Egea, M. A.; Garcia, M. L.; Souto, E. B. *Int J Pharm*, **2010,** 393(1–2), 168–176.

32. Silva, A. C.; Santos, D.; Ferreira, D. C.; Souto, E. B.; *Pharmazie*. **2009,** 64(3), 177–182.

33. Karade, P. G.; Shah, R. R.; Chougule, D. D.; Bhise, S. B. *Journal of Drug Delivery and Therapeutics*, **2012,** 2(3), 132-135.

34. Pandit, A. P.; Pol, V. V.; Kulkarni, V. S. *J Pharm*, **2016,** 3054321, 1–9.

35. Magnusson, B. M.; Cross, S. E.; Winckle, G.; Roberts. M. S. *Skin Pharmacol Physiol*, **2006,** 19 (6), 336-342.

36. Cirri, M.; Bragagni, M.; Menni, N.; Mura, P. *Eur J Pharm Biopharm*, **2011,** 32(4), 21-32.

37. Kaur, N.; Sharma, K.; Bedi, N. *Pharm Nanotechnol*, **2018,** 6, 133-143.

38. McClements, D. J. Food emulsions: Principles, practices, and techniques. CRC Press. United States, 2015.

39. Harde, H.; Agrawal, A. K.; Katariya, M.; Kale, D.; Jain, S. *RSC Adv*, **2015,** 5(55), 43917–4329.

40. Ranpise, H. A.; Gujar, K. N.; Mathure, D.; Satpute, P. P.; Awasthi, R.; Dua, K.; Madan, J. R.; *Pharm Nanotechnol*, **2018,** 6(3), 192-200.

41. Agrawal, Y.; Petkar, K. C.; Sawant, K. K. *Int J Pharm*, **2010,** 401(1–2), 93–102.

42. Muller, R. H.; Mader, K.; Gohla S. *Int J Pharm*, **2000,** 454(2), 154–161.

43. Radtke, M.; Müller, R. H.; *Pharm Teachnology Eur*, **1991,** 17(4), 1–4.

44. Müller, R. H.; Radtke, M.; Wissing, S. A. *Adv Drug Deliv Rev*, **2002,** 54, 131–155.

45. Nava, G.; Piñón, E.; Mendoza, L.; Mendoza, N.; Quintanar, D.; Ganem, A. *Pharmaceutics*, **2011,** 3(4), 954–970.

46. Teng, Z.,; Yu, M.; Ding, Y.; Zhang, H.; Shen, Y.; Jiang, M.; Liu, P. Opoku-Damoah, Y., Webster, T.J., Zhou, J., *Int J Nanomedicine*, **2019,** 14, 119–133.

47. Patwekar, S. L.; Pedewad, S. R.; Gattani, S. *Part Sci Technol*, **2018,** 36(7), 832–843.

48. Zhang, K.; Lv, S.; Li, X.; Feng, Y.; Li, X.; Liu, L.; Li, S.; Li, Y. *Int J Nanomedicine*, **2013,** 8, 3227–3239.

49. Shen, L. N.; Zhang, Y. T.; Wang, Q.; Xu, L.; Feng, N. P. *Int J Pharm*, **2014,** 460(1–2), 280–288.